HAL open science

Atmospheric loss of nitrous oxide (N2O) is not influenced by its potential reactions with OH and NO3 radicals

A R Ravishankara, Anne-Laure Pelé, Li Zhou, Yangang Ren, Antonia Zogka, Véronique Daële, Mahmoud S Idir, Steven P.Brown, Manolis N. Romanias, Abdelwahid S Mellouki

To cite this version:

A R Ravishankara, Anne-Laure Pelé, Li Zhou, Yangang Ren, Antonia Zogka, et al.. Atmospheric loss of nitrous oxide (N2O) is not influenced by its potential reactions with OH and NO3 radicals. Physical Chemistry Chemical Physics, 2019, 21, pp.24592-24600. 10.1039/C9CP04818A . insu-02373036

HAL Id: insu-02373036

https://insu.hal.science/insu-02373036v1

Submitted on 20 Nov 2019

HAL is a multi-disciplinary open access archive for the deposit and dissemination of scientific research documents, whether they are published or not. The documents may come from teaching and research institutions in France or abroad, or from public or private research centers.

L'archive ouverte pluridisciplinaire **HAL**, est destinée au dépôt et à la diffusion de documents scientifiques de niveau recherche, publiés ou non, émanant des établissements d'enseignement et de recherche français ou étrangers, des laboratoires publics ou privés.

Distributed under a Creative Commons Attribution - NonCommercial - NoDerivatives 4.0 International License

Atmospheric loss of nitrous oxide (N_2O) is not influenced by its potential reactions with OH and NO_3 radicals

A.R. Ravishankara,[*a,b,c] Anne-Laure Pele,[a] Li Zhou,[a,d] Yangang Ren,[a] Antonia Zogka,[a] Véronique Daële,[a] Mahmoud Idir,[a] Steven S. Brown,[e,f] Manolis N. Romanias,[g] and Abdelwahid Mellouki. [*a]

a. Institut de Combustion, Aérothermique, Réactivité et Environnement/OSUC, CNRS, 45071 Orléans Cedex 02, France.

b. Departments of Chemistry and Atmospheric Science, Colorado State University, Fort Collins, CO 80253, USA.

c. Le Studium Loire Valley Institute for Advanced Studies, Orléans, France.

d. Current Address: College of Architecture and Environment, Sichuan University, 610065 Chengdu, China.

e. National Oceanic and Atmospheric Administration, Earth System Research Laboratory, Chemical Sciences Division, 325 Broadway, Boulder, CO 80305, USA.

f. Department of Chemistry, University of Colorado, Boulder, CO 80309, USA.

g. IMT Lille Douai, Univ. Lille, SAGE 59000 Lille, France.

*Address correspondence to:

A.R.Ravishankara@colostate.edu or mellouki@cnrs-orleans.fr

Abstract

The rate coefficient for the possible reaction of OH radical with N_2O was determined to be $k_1 < 1 \times 10^{-17}$ cm^3 $molecule^{-1}$ s^{-1} between 253 and 372 K using pulsed laser photolysis to generate OH radicals and pulsed laser induced fluorescence to detect them. The rate coefficient for the reaction of NO_3 radical with N_2O was measured to be $k_2 < 5 \times 10^{-20}$ cm^3 $molecule^{-1}$ s^{-1} at 298 K using a direct method that involves a larger reaction chamber equipped with cavity ring down spectroscopic detection of NO_3 and N_2O_5. Various tests were carried out ensure the accuracy of our measurements. Based on our measured upper limits, we suggest that these two reactions alter the atmospheric lifetime of N_2O of ~120 years by less than 4%.

1. Introduction

Nitrous oxide, N_2O, is the third most important greenhouse gas[1] and is now the most important emission of an ozone layer depleting gas.[2] Nitrous oxide has both natural and anthropogenic sources.[3] All N_2O sources are spatially diffuse and emission rates from individual sources are low; therefore, it is difficult to quantify the emissions from individual sources. Our best estimate of the total emission of N_2O is based on measured atmospheric abundance (and growth rates) and estimated atmospheric lifetime of N_2O. Currently, the best estimate of the lifetime of N_2O is roughly 120 years.[4] Therefore, any error in the calculated atmospheric lifetime leads to a proportionate error in the overall emission rate and the estimated budget of N_2O. Such an error also propagates into the calculated ozone depletion potential and the global

warming potential of N_2O. The current estimate of the atmospheric lifetime of N_2O is based on its loss due to stratospheric removal via photolysis and reaction with $O(^1D)$. Even a small tropospheric loss rate due to reactions with oxidants such as OH and NO_3 would change the calculated atmospheric lifetime with consequences to the estimated emissions of N_2O, its atmospheric budget, its global warming potential and its ozone depletion potential. (The potential reaction of N_2O with O_3 has not been studied but is expected to be very slow.) Therefore, it is important to quantify all potential loss processes. This paper focuses on the potential reaction of N_2O with OH and NO_3 radicals, two of the ubiquitous oxidants in the troposphere.

The potential reactions of Cl and Br atoms with N_2O could also alter the lifetime of N_2O since there are non-negligible levels of Cl and Br in the troposphere as well as the stratosphere. The rate coefficients for the reactions of N_2O with Cl[5,6] and Br [6-8] have been examined at high temperatures by Lesar et al. They have also calculated the barrier heights for these reactions. Based on these results, it is unlikely that the reaction of Cl atoms would be a significant contributor to N_2O loss in the troposphere, where the Cl atom concentrations would be less than 1×10^4 cm^{-3} in the troposphere (see for example references 9,10) or the stratosphere where the concentrations are slightly larger[11] but temperatures are lower. Even though significant concentrations approaching ppt levels of Br have been observed in localized areas (See for example reference 10), they too are unlikely to contribute significantly. Further studies of the halogen reactions, especially measurements at atmospheric temperatures and more refined quantum calculations, may be warranted.

Previous studies have attempted to quantify the rate coefficients for the reactions of N_2O with OH and NO_3 radicals. Four previous studies attempted to measure the rate coefficient for the reaction of OH with N_2O:

$$\mathbf{OH + N_2O \xrightarrow{k_1} Products} \quad (1)$$

Chang and Kaufman[12]and Atkinson et al.[13] studied this reaction using the flow tube and flash photolysis techniques, respectively, and placed upper limits of < 4×10^{-16} and < 2×10^{-16} cm^3 $molecule^{-1}$ s^{-1}. Gordon and Mulac[14] placed an upper limit of < 1.7×10^{-14} cm^3 $molecule^{-1}$ s^{-1} using measurements done in a pulsed radiolysis experiment. Biermann et al.[15] reported rate coefficients for this reaction of k_1= $(3.8 \pm 1.2)\times10^{-17}$ and $(3.1 \pm 0.8)\times10^{-17}$ cm^3 $molecule^{-1}$ s^{-1} at 298 K and 283 K, respectively. Fleming et al.[16] have considered this reaction in an attempt to define lifetimes of N_2O and placed an upper limit of < 5×10^{-17} cm^3 $molecule^{-1}$ s^{-1} at 298 K. Clearly, this is a slow reaction, if it occurs at all. However, even the upper limit noted by Fleming et al. would reduce the atmospheric lifetime of N_2O by nearly 20 years and the calculated emissions would also be ~20% higher. Very recently, a theoretical study (which was carried out subsequent to the measurement reported here) has placed a very low value (<7×10^{-28} cm^3 $molecule^{-1}$ s^{-1}) for the rate coefficient for this reaction.[17]

The reaction of N_2O with NO_3

$$\mathbf{NO_3 + N_2O \xrightarrow{k_2} Products} \quad (2)$$

is also expected to be very slow. Cantrell et al.[18] reported an upper limit of $k_2 < 2 \times 10^{-17}$ cm^3 $molecule^{-1}$ s^{-1}. Again, such a rate coefficient would significantly alter the estimated lifetime of N_2O in the atmosphere. Similar to k_1, a theoretical study, carried

out subsequent to our measurements, places a very low value (3×10^{-43} cm^3 $molecule^{-1}$ s^{-1}) for the rate coefficient for this reaction[19].

Because rate coefficients for the reactions (1) and (2) are very small, their accurate determination is challenging. However, the analytical capability to measure small reaction rate coefficients, with little or no interferences from secondary reactions, has improved since the above upper limits were reported a few decades ago. For example, the use of pulsed laser photolysis to generate the OH radical and laser-induced fluorescence to detect them greatly enhanced our ability to minimize photolysis of N_2O and precisely detect OH in large concentrations of N_2O. Similarly, we have recently developed a method to study slow reactions of NO_3 by using cavity ring down spectroscopy coupled to a very large (7.3 m^3) chamber.[20, 21] Furthermore, our ability to measure and quantify impurities using various analytical techniques has improved over the past few decades. Therefore, we undertook this study to more accurately determine k_1 and k_2.

The reaction of OH with N_2O has two potential reactive pathways:[17]

$$\mathbf{OH + N_2O \xrightarrow{k_{1a}} HO_2 + N_2} \quad \text{(1a); } \Delta_r H^o(298\text{ K}) = -108.0 \text{ kJ mol}^{-1}$$[11]

$$\mathbf{OH + N_2O \overset{k_{1b}}{\leftrightarrow} OH \cdot N_2O} \quad \text{(1b); } \Delta_r H^o(0\text{ K}) = +55.2 \text{ kJ mol}^{-1}$$

Reaction 1b, which is reversible addition,[17] could be followed by abstraction of H by O_2 leading to the same final products, i.e., HO_2 and N_2. All other reaction pathways are very endothermic and are not important under atmospheric temperatures.

Similarly, the reaction of NO_3 with N_2O has only one exothermic channel:

$$N_2O + NO_3 \rightarrow N_2 + O_2 + NO_2;\ \Delta_r H^o(298\ K) = -122.4\ kJ\ mol^{-1} \quad (2a)$$

The other possible reactions are endothermic:

$$N_2O + NO_3 \rightarrow 2NO + NO_2;\ \Delta_r H^o(298\ K) = +59.71\ kJ\ mol^{-1} \quad (2b)$$

and

$$N_2O + NO_3 \rightarrow N_2O + NO + O_2;\ \Delta_r H^o(298\ K) = +16.34\ kJ\ mol^{-1} \quad (2c)$$

Reactions 2b and 2c are endothermic but could be facilitated by the large entropy change. The endothermic Reaction 2c, if it occurs at all, will not lead to N_2O loss; it serves to catalyze NO_3 decomposition.

Here, we report the upper limits for the rate coefficient for the reactions of OH and NO_3 with N_2O and quantify the contributions of these two reactions to the loss of N_2O in the troposphere. By this quantification, we are able to better constrain the atmospheric lifetime of N_2O and, hence, its budget.

2. Experimental Section

We measured the rate coefficient for the reaction of OH with N_2O by following its temporal profile via pulsed laser induced fluorescence subsequent to its pulsed-photolytic production in an excess of N_2O. We followed the temporal profile of NO_3 (and N_2O_5 in equilibrium with NO_3) via cavity ring down spectroscopy (CRDS) in the presence of an excess of N_2O in a large atmospheric simulation chamber. The experimental apparatuses, the procedures, and data analyses are different for these two reactions. Therefore, we will describe them separately.

2.1 Measurement of the rate coefficient for the reaction of OH with N_2O

The apparatus used to measure OH reaction rate coefficients via pulsed photolysis have been described in detail in many previous studies[22] and the specific apparatus used here is also described previously [23]. Therefore, we describe only few details necessary to understand the present study. Further details, including the schematic of the apparatus (Fig. S1), are given in the Supplementary Information.

The apparatus consisted of a jacketed Pyrex cell (volume = 200 cm^3) through which N_2O, H_2O_2 (used as the OH precursor), and a bath gas (mostly Ar) were introduced using calibrated mass flow controllers. Water (for temperature above 298 K) or pure ethanol (for temperatures below 298 K) was flowed through the outer jacket of the reactor to achieve the desired temperature (T = 253 - 372 K). The temperature of the gas mixture flowing through the reactor in the reaction zone (defined as the volume where the photolysis and the probe beams intersect) was measured using a retractable thermocouple.

H_2O_2 was photolyzed by a 248 nm KrF excimer laser to produce an initial OH concentration, $[OH]_0$, of typically around 10^{11} cm^{-3}. A Nd: YAG-pumped frequency-doubled dye laser was used to excite the OH radical ($X^2\Pi$ v”=0 $\rightarrow$ ($A^2\Sigma^+$ v’=1) at $\lambda \cong 282$ nm. The resulting fluorescence around 308 nm from ($A^2\Sigma^+$ v’=1) $\rightarrow$ ($X^2\Pi$ v”=1) and ($A^2\Sigma^+$ v’=0) $\rightarrow$ ($X^2\Pi$ v”=0) was then detected by a photomultiplier tube positioned orthogonally to the two laser beams. The signal from the PM tube was processed through a gated charge integrator and fed to a

computer. The time delay between the excimer and probe lasers were varied to change the reaction time.

The determination of the rate coefficient of a very slow reaction is challenging mainly because we need to use very high concentrations of N_2O, the excess reagent. The high concentrations of N_2O very rapidly quench the OH fluorescence signal. The collected OH fluorescence was first passed through a bandpass filter centered at 310 nm with a full width at half maximum (FWHM) of 10 nm (with transmission >70% at 310 nm) before reaching the photomultiplier tube. Scattered light from the 282 nm laser beam inside the cell (and any fluorescence it caused in the cell), was reduced almost to undetectable levels by rotating the beam polarization from horizontal to vertical with a $\lambda/2$ wave plate before entering the cell, installing an exit window at Brewster angle and dumping the beam into a beam dump to minimize back scatter. This arrangement greatly reduced the scattered light and we could detect 1×10^9 OH cm^{-3} for integration of 100 pulses in 50 torr of N_2O with a signal to noise of unity.

All experiments were carried out under pseudo-first order conditions in [OH] by maintaining the concentrations of N_2O much larger than $[OH]_0$, the initial hydroxyl radical concentrations; i.e., $[N_2O] >> [OH]_0$. The temporal profiles of [OH], therefore, followed a first order rate law:

$$[OH]_t = [OH]_0 e^{-k't}; \text{ where } k' = k_1[N_2O] + k'_0 \qquad \text{(I)}$$

k' is the first-order decay rate, k_1 is the bimolecular rate coefficient for reaction (1). k'_0 is the rate coefficient for OH removal in the absence of N_2O; it

is expressed as a first order rate coefficient. This loss process is due to a combination of diffusion of OH out of the reaction zone and reactions of OH with H_2O_2 and impurities in the bath gas. The concentration of OH at various reaction times were determined by changing the delay between the photolysis and probe lasers, recording the fluorescence signal at 10 to 20 different delay times and averaging signals from up to 300 probe laser pulses for each delay time. The LIF signal detected by the photomultiplier tube was captured using homemade electronics and a LabView program. A non-linear least-squares analysis was used to fit the fluorescence signal versus time data to Equation (I) to extract the values of k'. The second-order rate coefficients were obtained from linear least squares analysis of the k' values determined at various N_2O concentrations. Typical first order fluorescence signal and plots of k' vs [N_2O] are shown in the Supplementary Information.

Both the photolysis and probe lasers were operated at 10 Hz and their energies were measured by laser power monitors situated at the exits of the cell, (13-44) mJ cm^{-2}. They remained constant during the course of measuring a given OH temporal profile. Between 2 and 55 Torr of N_2O was added to a large flow of Ar for a total pressure of 500 Torr in the reactor. This mixture was flowed through the reaction cell (0.09 to 27 cm s^{-1}) such that a given aliquot of the gas mixture was exposed to only a few laser pulses; most often, they were exposed to only one photolysis laser pulse.

The concentrations of gases inside were calculated from the measured flow rates of gases using calibrated electronic mass flow controllers and the measured temperature and pressure in the reaction cell. Pressure was determined using a calibrated capacitance manometer. The electronic mass flow meters were calibrated by measuring the rate of pressure rise when a given gas flowed through the mass flow controller into a known volume. Partial pressures of the gases were computed from the mass flow rates and the total cell pressure. The estimated uncertainty in N_2O concentration in the reactor is better than 5%.

2.2 Measurement of rate coefficient for the reaction of NO_3 with N_2O

The rate coefficient for the reaction of NO_3 with N_2O was measured at room temperature (298.0 ± 1.5K) in the ICARE-7300L Teflon chamber and at atmospheric pressure (1000 ± 5 hpa) (shown in the Supplementary Information as Fig. S2). This chamber, the CRDS detection of NO_3 and N_2O_5, the related gas handling system, and the procedures used to measure rate coefficients have been described in detail in our previous work.[24, 25] The method and procedure used here were very similar to those described earlier. Therefore, only information necessary to understand the present work is given here.

During kinetics studies, a flow (about 10 L min^{-1}) of purified air was added to maintain the chamber slightly above atmospheric pressure and compensate for the pressure reduction caused by the continuous withdrawal of the gas mixture from the chamber for analysis. Maintaining the pressure slightly above ambient also prevented

any room air from leaking into the chamber. The chamber contents were mixed by two fans within the chamber. The dilution rate and mixing time in the chamber were measured by injecting a sample of SF_6 (> 99.99%, Alpha Gaz) into the chamber and measuring its temporal profile using a FTIR spectrometer. In this study, the dilution rate (expressed as a first order rate coefficient) was 2.3×10^{-5} s^{-1} and the mixing time (for > 99% mixing) was less than 30s. The key analytical instruments used in this study are the commercial Nicolet 5700 Magna FT-IR spectrometer and a two-channel Cavity Ring Down Spectrometer.[25] The IR spectra of the gas mixture in the chamber were recorded by co-adding 16 scans at a spectral resolution of 1 cm^{-1} (path length of 140 m). The time resolution with this measurement was 2 mins. N_2O and SF_6 were monitored, respectively, at 2620 cm^{-1} - 2410 cm^{-1} and 954 cm^{-1} - 934 cm^{-1}. The integrated absorbances (peak areas) were used for calibration (See Fig. S3) which enabled determining the concentrations of N_2O in the reactor.

A two-channel cavity ring down spectrometer operating at 662 nm was used to simultaneously measure the concentrations of NO_3 (in one channel) and N_2O_5 + NO_3 (in another channel). The time resolution of the instrument was 1s with detection sensitivities of roughly 0.4 and 2 pptv for NO_3 and N_2O_5 for 1 second integration, respectively, as described in detail by Fuchs et al.[26] Since we used roughly a ppbv of NO_3 and a few ppbv of N_2O_5, the signal to noise ratios for kinetics experiments were excellent. The gas sample entering the CRDS system was passed through a filter to remove any aerosols present in the chamber and thus minimize scatter of the 662 nm light that degrades the signal. The total loss of NO_3 and N_2O_5 to the walls of the CRDS

instrument and the filter have been estimated[26-28] to be less than 20% and 4%, respectively, for NO_3 and N_2O_5; these losses were accounted for in calculating the concentrations. The uncertainties in measuring the concentrations and rate coefficients are described in previous publications.[25] As described previously, even though we studied reaction 2 under pseudo first order conditions in NO_3, we need the absolute concentration since NO_3 is tightly coupled to N_2O_5 in the system through its equilibrium,

$$N_2O_5 \xrightarrow{k_3} NO_3 + NO_2 \qquad (3)$$

$$NO_3 + NO_2 \xrightarrow{k_4} N_2O_5 \qquad (4)$$

The rate coefficients for the reactions of NO_3 radicals with N_2O were measured by following the temporal profiles of NO_3 and N_2O_5 in an excess of N_2O. The rate coefficient k_2 was obtained by simultaneously fitting the temporal profiles of NO_3 and N_2O_5.

First, N_2O_5 was injected into the chamber to generate NO_3 (and NO_2). An equilibrium among NO_3, NO_2, and N_2O_5 (Reactions 3 and 4 below) was set up rapidly and maintained throughout the course of kinetics studies. The initial mixing ratios of N_2O_5 were varied between 8 and 25 ppbv and the resulting initial mixing ratios of NO_3 were between 0.5 and 2.5 ppbv. The concentrations of NO_3 and N_2O_5 were measured for 10 mins to observe their losses in the chamber due to wall loss, dilution, and reactions with any impurities. The measured temporal profiles were fit by using a model that integrated the following set of reactions occurring in the chamber to derive the time dependence of NO_3, N_2O_5 and NO_2, as described previously:[25]

$$N_2O_5 \xrightarrow{k_3} NO_3 + NO_2 \qquad (3)$$

$$NO_3 + NO_2 \xrightarrow{k_4} N_2O_5 \qquad (4)$$

$$NO_3 \xrightarrow{k_5} \text{loss} \qquad (5)$$

$$N_2O_5 \xrightarrow{k_6} \text{loss} \qquad (6)$$

The fitting was carried out by simultaneously minimizing the sum of least-squares for both NO_3 and N_2O_5 profiles by changing the initial concentrations of each reactant and reaction rate coefficients of each reaction as input parameters. The values of the rate coefficients for the reactions involved in the equilibrium are well known. The equilibrium constant, $k_{eq} = [N_2O_5]/[NO_3][NO_2] = k_4/k_3$, k_3, and k_4 were taken from NASA/JPL recommendation.[11] We varied k_4 by less than 5% to improve the fits since a small uncertainty in temperature makes a significant difference in the fit. However, the equilibrium constant that was used was always within 5%, the difference expected for a temperature variation of about 0.5 K. Using this procedure, the best values for the loss rate coefficients k_5 and k_6 in the absence of N_2O (usually termed "wall loss rate coefficients") were derived from the fit.

Once the data for wall loss rate coefficients were derived, a known concentration of N_2O (from FTIR measurements) was added to the chamber and the loss rates of N_2O_5 and NO_3 were monitored for up to 60 mins.

$$N_2O + NO_3 \xrightarrow{k_2} \text{Products} \qquad (2)$$

The measured profiles of NO_3 and N_2O_5 were again fit by varying k_2 while keeping all the other rate coefficients the same as those determined in the previous steps. The best

value of the rate coefficient was obtained by fitting both NO_3 and N_2O_5 profiles (i.e., by minimizing the sum of least-squares for both NO_3 and N_2O_5 profiles simultaneously).

2.3 Materials used in this study

Argon (> 99.9999%, Air Liquide) and SF_6 (> 99.999%, Air Liquide) were used without further purification. Two samples of N_2O (from Air Liquide) with stated purities of 99% (industrial) and 99.998% were used for all experiments. Since impurity levels in the N_2O samples were not given by the vendors, we analysed them using a Proton Transfer Reaction Time-of-Flight Mass spectrometer (Ionicon PTR-ToF-MS 8000) for reactive hydrocarbons, Fourier Transform Infrared Spectroscopy (Thermo-Fischer FTIR) for hydrocarbons and other potential impurities such as CO and CO_2, Cavity Ring-Down Spectroscopy (CRDS), a NOx monitor, and an Aerodyne CAPS NO_2 monitor for NO_2. The measured impurity levels were: H_2O < 3 ppm, O_2 < 2 ppm, C_nH_m < 1 ppm, CO < 1 ppm, CO_2 < 2 ppm, H_2 < 0.1 ppm (specified by vendor), N_2 < 10 ppm (specified by vendor), NO_x ($NO+NO_2$) < 1ppb, and NO_2 < 1 ppm. It should be noted that any NO would be quickly removed in the experiments involving NO_3 and thus would not affect the N_2O rate coefficient measurement. Details are given in the SI. N_2 had a stated purity of (> 99.9999%, Air Liquide) and was used as supplied. A 35 wt.% H_2O_2 solution was obtained from Prolabo and was concentrated by bubbling helium (Air Liquide, ≥ 99.9999%) through the solution for several days prior to use to remove water and obtain concentrated (~ 90%) H_2O_2. Either Ar or N_2 was flowed constantly through the H_2O_2 sample to keep it as pure as possible. Pure N_2O_5 was

synthesized by mixing NO with O_3 in a slow flow and collecting N_2O_5 in a trap at 193 K and purifying the sample, as described by Davidson et al.[29].

3. Results and Discussion

In this study we measured k_1 and k_2 using two experimental apparatuses. The methods used for the analyses of the two rate coefficients are different. Further, the previous studies of these two reactions come from studies that were essentially focused on OH reaction or NO_3 reactions. Therefore, we will present and discuss the results of the two reaction rate coefficients separately.

3.1 Reaction of OH with N_2O

As a test of our ability to measure small rate coefficients, we first measured the well-known rate coefficient for the reaction OH with CH_4:

$$OH + CH_4 \xrightarrow{k_7} CH_3 + H_2O \quad ; \quad (7)$$

We obtained a value of $k_7 = (6.19 \pm 0.04) \times 10^{-15}$ cm^3 molecule^{-1} s^{-1} (2 σ precision only) at 298 K. When we include the uncertainty in the measurement of CH_4 concentration, we obtained a value of $k_7 = (6.19 \pm 0.31) \times 10^{-15}$ cm^3 molecule^{-1}s^{-1}, in excellent agreement with the current recommendations of NASA/JPL[11] and IUPAC panels[30], respectively, of 6.3×10^{-15} and 6.4×10^{-15} cm^3 molecule^{-1} s^{-1}. It is also in excellent agreement with the original measurements of Vaghjiani and Ravishankara[22] of $(6.25 \pm 0.12) \times 10^{-15}$ cm^{3}molecule^{-1}s^{-1} as well as that of Mellouki et al.,[23] $(6.34 \pm 0.56) \times 10^{-15}$ cm^{3}molecule^{-1}s^{-1}, using a previous version

of the apparatus used here. Therefore, we are confident of our OH reaction kinetics capabilities.

The measured OH loss temporal profiles in the presence of N_2O were always exponential (Fig. S4). A high pressure of Ar (500 Torr) was used as a bath gas for all measurements. Use of Ar, which does not quench OH fluorescence significantly, reduced the changes in diffusive loss of OH when large concentrations of N_2O were added to the reactor. Fig. 1 shows a plot of the measured pseudo-first-order rate coefficient for the loss of OH as a function of N_2O concentration at 253, 298 and 372 K. For greater clarity the data obtained at 372 K is shown in the inset to the figure. Clearly, the slopes of these plots are negative and statistically different from zero. We attribute this slightly negative value to the reduction in OH loss rate from the reaction zone as N_2O concentration increases (even in the presence of 500 Torr of Ar) and further hinders diffusion out of the reaction zone. To test this hypothesis, we replaced N_2O by N_2, which does not react with OH but has a larger collision diameter than Ar to reduce the diffusion out of the reaction zone. Clearly, we see a very similar behaviour of decreasing k' with increasing N_2 concentrations. Furthermore, use of He in preliminary experiments showed much larger decreases in k' upon addition of N_2O. These observations add confidence to our attribution of the negative value of the slope to the reduced diffusive loss of OH when N_2O is added to the reactor.

The only way to observe a negative rate coefficient is for a slow generation of OH (more than what is consumed by reactions with H_2O_2 and impurities) due to some reaction subsequent to the photolytic production OH in the presence of

N_2O. The quantum yield for the production of OH in the photodissociation of H_2O_2 is known to be 2.[11] Other potential radicals that could be produced are O (from N_2O or H_2O_2 photolysis),[11] atoms and HO_2 radicals (from H_2O_2 photolysis).[31] With the known quantum yields for the production of O, H, and HO_2, we estimate that at most 10^8 cm^{-3} of these reactive species could be produced in our system. The contribution of N_2O photolysis is negligible (either via one or two photon dissociation). These radicals are not known to react rapidly with N_2O or with H_2O_2. Even if they did, their concentrations are such that they could not influence the measured temporal profiles. To experimentally check for this possibility, we varied the photolysis laser fluence, initial OH concentration, H_2O_2 concentration, and linear flow velocity of the gas through the reactor. The obtained values of k_1 were independent of these variations, demonstrating the absence of significant errors due to secondary reactions in our measurements.

There are other potential reactions that could lead to the slow regeneration of OH. The HO_2 radical (produced by OH reaction with H_2O_2) could react with O, H, or NO (either present as an impurity in N_2O or produced via photolysis of N_2O followed by the reaction of $O(^1D)$ with N_2O). Therefore, we carefully measured the NO impurity in N_2O and found it to be less than 1 ppbv; therefore the concentration of NO in the reaction mixture was no more than 0.1 ppbv (or $<2.5 \times 10^9$ cm^{-3}) in the reactor. The photolytic production of NO from the 248 nm photolysis of N_2O was calculated to be less than 2×10^{11} cm^{-3} at the laser fluences used here. Even if this level of NO were generated, it could not

reproduce OH during the time scale of the measurements. Furthermore, we varied the laser fluence by almost a factor of 3 with no discernible (<5%) changes and within the precision of our measurements). This test also excludes any two-photon photolysis of N_2O that could generate NO. Similarly, the calculated O and H atoms concentrations are $<10^8$ cm^3. To check for any such secondary reactions, we modelled a set of reactions shown below.

$$OH + H_2O_2 \rightarrow H_2O + HO_2 \quad (8)$$

$$OH + HO_2 \rightarrow H_2O + O_2 \quad (9)$$

$$OH \rightarrow \text{loss by diffusion} \quad (10)$$

$$OH + N_2O \rightarrow HO_2 + N_2 \quad (1)$$

$$N_2O + h\nu \rightarrow N_2 + O(1D), \lambda < 337 \text{ nm} \quad (11)$$

$$O(1D) + H_2O \rightarrow 2OH \quad (12)$$

$$O(1D) + N_2O \rightarrow 2NO \quad (13a)$$

$$O(1D) + N_2O \rightarrow N2 + O2 \quad (13b)$$

$$NO + HO_2 \rightarrow OH + NO_2 \quad (14)$$

The results showed that we could not regenerate OH in the time scale of our experiments. The contributions of other reactive impurities, if present, would only lead to an over estimation of the measured rate coefficient.

We obtained the upper limits for the rate coefficients at each temperature by fitting all pseudo-first-order rate coefficients at a given temperature to a straight

line using unweighted linear least squares routine and then adding the 2σ uncertainties in the fit (Table 1). Table 1 lists the slopes of the plots shown in Fig. 1 (k_1) along with the experimental conditions used in their determination. An alternative way to estimate the rate coefficient is to compare the measured "negative" rate coefficient with that measured with N_2 (a non-reacting molecule). We took the difference between values measured in N_2O with that in N_2 and added twice the standard deviations in the measured value to the difference. This approach yields k_1 = (6.0 ± 2.6) × 10^{-18} and (4.2 ± 0.7) × 10^{-18} cm^3 $molecule^{-1}$ s^{-1} at 253 K and 298 K, respectively. Therefore, we suggest that the upper limit for the rate coefficient for this reaction is k_1 <1 × 10^{-17} cm^3 $molecule^{-1}$ s^{-1} at all the temperatures measured.

Table 1. Summary of experimental conditions and measured values for the rate coefficients, k_1 (T), for the OH + N_2O reaction. These values are denoted with an asterisk since we attribute them to effect of N_2O on OH diffusion rather than reaction with OH.

T (K)	Pressure of Ar (Torr)	$[N_2O]$ (10^{17} cm^{-3})	$[H_2O_2]$ (10^{13} cm^{-3})	$[OH]_0$ (10^{11} cm^{-3})	Fluence mJ cm^{-2}	k_1 (10^{-17} cm^3 $molecule^{-1}s^{-1}$)	
						Measured	Upper limit
253	500 (99%)	0.62-14.30	2.12-3.75	0.81-1.42	17	-0.91 ± 0.39	< 0.88
253	500 (99.998%)	1.41-10.52	3.18-3.89	3.12-3.82	16		
298	500 (99%)	0.44-17.60	2.57-4.22	2.42-3.96	34-44	-1.09 ± 0.34	< 0.49
298	500 (99.998%)	1.27-10.42	3.50-4.40	3.44-4.32	17		
372	500 (99%)	0.44-8.52	3.00-5.40	2.21-5.30	33-44	-2.26 ± 1.34	< 0.38

372	500 (99.998%)	1.41-6.57	3.45-4.19	3.38-4.11	13

All quoted uncertainties are 2σ from the precision of the least-squares analysis of k' versus [N_2O].

Comparison with literature values: Gordon and Mulac[14] followed the temporal profile of OH via resonance absorption following pulsed radiolytic production of OH in the presence of N_2O and reported an upper limit of $k_1 < 1.7\times10^{-14}$ cm^3 $molecule^{-1}$ s^{-1} at 440 K. Atkinson et al.[13] reported an upper limit of $< 2\times10^{-16}$ cm^3 $molecule^{-1}$ s^{-1} at both 298 K and 442.8 K using the pulsed photolysis-resonance fluorescence technique. Chang and Kaufman[12] failed to measure an observable enhancement in OH loss rates in the presence of N_2O in their flow tube reactor and place an upper limit of $<4\times10^{-16}$ cm^3 $molecule^{-1}$ s^{-1}. Our values are lower than these three reports but consistent with them given that they are all upper limits.

However, Biermann et al.[15] reported $k_1= (3.8 \pm 1.2)\times10^{-17}$ and $(3.1 \pm 0.8)\times10^{-17}$ cm^3 $molecule^{-1}$ s^{-1} at 298 K and 283 K, respectively. They used long path resonance absorption detection of OH subsequent to its production via water photolysis using a synchronized bank of flash lamps in their long cell. They reported that the measured first order rate coefficients for the loss of OH increased linearly with N_2O concentration and derived the values noted above. Our results are not consistent with this reported rate coefficient. We suspect that N_2O was photolyzed in their reactor since they used LiF windows on their photolysis lamps that would have allowed photolysis wavelengths down to ~115 nm into their reactor. With the short wavelength radiation,

N_2O would have been photolyzed and the subsequent reaction of $O(^1D)$ with N_2O would produce NO. Since they used Ar as the bath gas, only a small fraction of the $O(^1D)$ would have been quenched and large concentrations of NO would have been produced. (Note that the rate coefficient for the quenching of $O(^1D)$ by Ar is about 100 times smaller than that by N_2O). The extent of NO production would increase linearly with N_2O concentration such that it could appear that the measured first order rate coefficient for the loss of OH increased with N_2O abundance. We cannot accurately calculate the extent of NO production in their system but based on their reported initial concentration of $[OH]_0$ and water vapor pressure, we suspect that more than 1×10^{13} cm^{-3} of NO would have been produced in 75 Torr of N_2O per photolysis flash. If they could generate as much as 1×10^{14} cm^{-3} of NO, the reaction of OH with NO would account for their observed OH loss rates, increasing linearly with increasing N_2O concentration as NO production increased and OH loss increased due to the reaction of NO with OH. However, for this explanation, the third body efficiency of N_2O in the OH + NO + M reaction has to be similar to that of Ar (otherwise, they would have likely seen a quadratic dependence on N_2O abundance). In the absence of detailed information on the experimental conditions hinders better estimates of this interference. We do note that the experiments of Biermann et al. were the state of the art about 40 years ago and they did their best to obtain the rate coefficient for a slow reaction.

Very recently, the theoretical calculations of Nguyen et al. placed an upper limit for the rate coefficient for OH reaction with N_2O to be ($<7\times10^{-28}$ cm^3 $molecule^{-1}$ s^{-1}).

Our measured upper limit is much larger than that calculated by Nguyen et al. but, being an upper limit, it is consistent with their estimates.

3.2 Reaction of NO_3 with N_2O

Fig. 2 shows the measured temporal profiles of NO_3 and N_2O_5 mixing ratios in the chamber in the presence of N_2O along with the fits of the profiles to a reaction scheme consisting of Reactions 2 through 6. With the known values of the rate coefficients for Reactions 3 and 4, and the known initial concentrations of NO_3, N_2O_5 and NO_2 (the initial concentration of NO_2 was derived from k_{eq}), the values of k_5 and k_6 were derived from the fits to profiles (1) and (2). As noted in our earlier papers,[25] the fits were carried out by simultaneously minimizing the sum of squares of the residuals for both profiles. Subsequent to the addition of N_2O (lower traces 3 and 4), the profiles were again fit to extract k_2.

Experiments were carried out with different initial concentrations of N_2O and two samples of N_2O (99% and 99.998% purities). The uncertainty in the obtained values of k_2 due to fitting was very small, often much less than 5%. The uncertainty in the precision of our measured rate coefficient were obtained by the standard deviation of the mean of multiple measurements and including the Student t value for the limited number of measurements. The results of our measurements for N_2O are given in Table 2.

Table 2. Summary of the experimental conditions and rate coefficients for reaction of NO_3 with N_2O at (298.0 ±1.5) K.

N_2O purity	Initial mixing ratio				k_2[a]	k_2[b] incl. systematic errors
	N_2O (ppmv)	NO_3 (ppbv)	N_2O_5 (ppbv)	NO_2 (ppbv)	10^{-20} cm^3 $molecule^{-1}$ s^{-1}	
	867	0.38	6.75	21.76	5.00	
	819	0.52	10.47	25.17	5.50	
	2148	0.39	6.81	22.27	2.12	
99%	2040	0.59	11.55	25.08	1.70	
	2707	0.39	7.46	21.96	1.08	
	2439	0.39	8.05	24.02	1.10	
				Average	2.75±2.08	2.75±2.20
	2277	0.11	3.24	18.62	2.62	
	2214	0.49	14.84	19.83	1.01	
99.998%	3201	0.12	4.04	22.64	3.78	
	2386	0.17	4.54	18.21	3.45	
	2320	0.34	9.85	19.55	2.97	
				Average	2.77±1.34	2.77±1.52

[a] The k_2 values shown were derived by simultaneously fitting the observed profiles of NO_3 and N_2O_5 to a least squares algorithm. The quoted errors are at the 95% confidence level and indicate the precision of our measurements. It also accounts for limited number of measurements by using the Student t-distribution contribution.

[b] The quoted errors include estimated systematic errors as described in the text.

The errors in k_2 from: (1) the precision in the measurements of NO_3, N_2O_5 and N_2O; (2) the uncertainty of the rate coefficients used in the reaction schemes used in the fitting; (3) the precision of curve fitting; and (4) the presence of reactive impurities in the sample of the reactants.

In the present study, the systematic errors in measurements of NO_3 and N_2O_5 using the CRDS system employed here have been assessed to be −8/+11% for NO_3 and −9/+12% for N_2O_5, as noted earlier. Systematic errors in the measured concentration of the N_2O are estimated by using the uncertainty of the slope in the calibration plot (< 1%) and the uncertainty in measuring reactants concentration for the calibration (5%), both at the 95% confidence level. We simply added these two errors together to get the estimated uncertainty in the concentration of N_2O in the chamber since they could be correlated. The overall estimated error was calculated by adding in quadrature the fitting error, estimated contribution of absolute concentrations of NO_3 and N_2O_5, the precision of k_2 from the fitting routine, and the estimated uncertainty in the concentration of the N_2O. The uncertainty in the fitting, as noted above, is better than 5%. The uncertainty of the rate coefficients used in the reaction scheme is around 10%.[11] Table 2 lists the uncertainties in the measured values of k_2 along with the estimated systematic errors.

Another potential source of error in the measured value of k_2 is the presence of reactive impurities in the samples of N_2O. Two cylinders of N_2O with different stated purities (99% and 99.998%) were used. The derived rate coefficients for these two sources of N_2O are similar (Table 2) since the main impurities are unreactive chemicals such as, N_2, O_2, and CO_2. We do not believe that our reported values were greatly affected by the presence of reactive impurities. Yet, our reported values should be treated as the upper limits of k_2 since it is a very slow reaction and we recommend $k_2 \leq 5\times10^{-20}$ cm^3 $molecule^{-1}$ s^{-1} at T = (298.0 ± 1.5) K and (1000 ± 5) hpa of air.

Comparison with literature values: This reaction has been subject to only one previous investigation. Cantrell et al.[18] studied this reaction in a 450L Pyrex cell at room temperature. They did not observe loss of N_2O through NO_3 reaction and reported an upper limit of 2×10^{-17} cm^3 $molecule^{-1}$ s^{-1}. The upper limit of k_2 we obtained is about two orders of magnitude smaller.

3.3 Calculated reaction pathways and barrier

The potential energy surface for the reaction of N_2O with OH and NO_3 radicals were calculated as a part of this study. However, since those calculations, the energetics and reaction paths have been calculated and reported by Nguyen et al.[17, 19] Therefore, we have just shown the calculated potential energy surfaces in the Supplementary Information.

4. Atmospheric significance of measured rate coefficients

Our results show that the reactions of OH and NO_3 with N_2O are very slow. Using the upper limit for k_1 reported here, we estimate that the atmospheric lifetime of N_2O is reduced by at most 4% to 116 yr., from the currently used 120 yr. (This calculation assumes that the globally and diurnally average tropospheric OH abundance is 1×10^6 cm^{-3}). Theoretical calculations of k_1 by Nguyen et al. suggests that the influence of the OH reaction with N_2O is negligibly small in the atmosphere. Our upper limit for k_2 suggests that the contribution of Reaction (2) negligible. Even if we assume a globally average NO_3 concentration of 1×10^7 cm^{-3}, a quantity that remains undefined to date, the contribution of this reaction would be at most 0.2% to the calculated N_2O lifetime. Therefore, we suggest that Reactions (1) and (2) do not contribute to the calculated

lifetime of N_2O. It is interesting to note that the tropospheric loss of N_2O via its reaction with $O(^1D)$, present at very small concentration of <0.1 cm^{-3}, would contribute more to N_2O loss than either OH or N_2O reactions!

Acknowledgment: This work was carried out at CNRS in Orléans, France. It was supported by Labex Voltaire (ANR-10-LABX-100-01), the European Union's Horizon 2020 research and innovation programme through the EUROCHAMP-2020 Infrastructure Activity under grant agreement No. 730997, and ARD PIVOTS program (supported by the Centre-Val de Loire regional council). Europe invests in Centre-Val de Loire with the European Regional Development Fund. ARR acknowledges the Le Studium Advanced Institute of Loire Valley for a Research Professorship.

References

1. G. Myhre, D. Shindell, F.-M. Bréon, W. Collins, J. Fuglestvedt, J. Huang, D. Koch, J.F. Lamarque, D. Lee, B. Mendoza, T. Nakajima, A. Robock, G. Stephens, T. Takemura and H. Zhang,Anthropogenic and Natural Radiative Forcing. In: Climate Change, *The Physical Science Basis. Contribution of Working Group I to the Fifth Assessment Report of the Intergovernmental Panel on Climate Change*, 2013.
2. A. R. Ravishankara, J. S. Daniel and R. W. Portmann,Nitrous Oxide (N_2O): The Dominant Ozone-Depleting Substance Emitted in the 21st Century, *Science*, 2009, **326**, 123-125.
3. UNEP,Drawing Down N_2O to Protect Climate and the Ozone Layer. A UNEP Synthesis Report., *United Nations Environment Programme (UNEP), Nairobi, Kenya*, 2013.
4. P. N. M. Ko, S. Reimann, S. Strahan,SPARC Report on the Lifetimes of Stratospheric Ozone-Depleting Substances, Their Replacements, and Related Species, *SPARC Report No. 6, WCRP-15*, 2013.
5. A. Lesar, M. Hodošček and M. Senegačnik, Experimental and theoretical studies of the decomposition of N_2O catalyzed by chlorine, *J. Chem. Phys.*, 1996, **105**, 917-926.
6. A. Lesar and M. Hodoscek, Transition State Structure and Energetics of the N_2O + X (X = Cl,Br) Reactions, *J. Chem. Inf. Comput. Sci.*, 2002, **42**, 706-711.

7. A. Lesar and M. Senegačnik, ^{15}N and ^{18}O kinetic isotope effects in the thermal decomposition of N_2O catalyzed by bromine, *J. Chem. Phys.*, 1993, **99**, 187-195.

8. A. Lesar and M. Hodošček, Ab initio molecular orbital and density functional characterization of the potential energy surface of the N_2O+Br reaction, *J. Chem. Phys.*, 1998, **109**, 9410-9416.

9. X. Wang, D. J. Jacob, S. D. Eastham, M. P. Sulprizio, L. Zhu, Q. Chen, B. Alexander, T. Sherwen, M. J. Evans, B. H. Lee, J. D. Haskins, F. D. Lopez-Hilfiker, J. A. Thornton, G. L. Huey and H. Liao, The role of chlorine in global tropospheric chemistry, *Atmos. Chem. Phys.*, 2019, **19**, 3981-4003.

10. W. R. Simpson, S. S. Brown, A. Saiz-Lopez, J. A. Thornton and R. von Glasow, Tropospheric Halogen Chemistry: Sources, Cycling, and Impacts, *Chem Rev.*, 2015, **115**, 4035-4062.

11. S. P. Sander. J. B. Burkholder, J. P. D. Abbatt,J. R. Barker,R. E. Huie,C. E. Kolb,M. J. Kurylo,V. L. Orkin,D. M. Wilmouth,P. H. Wine,Chemical Kinetics and Photochemical Data for Use in Atmospheric Studies, 2015.

12. J. S. Chang and F. Kaufman,Upper limits of the rate constants for the reactions of $CFCl_3$(F-11), CF_2Cl_2(F-12), and N_2O with OH. Estimates of corresponding lower limits to their tropospheric lifetimes, *Geophys. Res. Lett.*, 1977, **4**, 192-194.

13. R. Atkinson, R. A. Perry and J. N. Pitts,Kinetics of the reactions of OH radicals with CO and N_2O, *Chem. Phys. Lett.*, 1976, **44**, 204-208.

14. S. Gordon and W. A. Mulac, *Reaction of the OH(X/sup 2/II) radical produced by the pulse radiolysis of water vapor*, ; Argonne National Lab., IL, 1975.

15. H. W. Biermann, C. Zetzsch and F. Stuhl,Rate Constant for the Reaction of OH with N_2O at 298 K, *Berichte der Bunsengesellschaft für physikalische Chemie*, 1976, **80**, 909-911.

16. E. L. Fleming, C. George, D. E. Heard, C. H. Jackman, M. J. Kurylo, W. Mellouki, V. L. Orkin, W. H. Swartz, T. J. Wallington, P. H. Wine and J. B. Burkholder,The impact of current CH_4 and N_2O atmospheric loss process uncertainties on calculated ozone abundances and trends, *J. Geophys. Res.: Atmos.*, 2015, **120**, 5267-5293.

17. T. L. Nguyen, A. R. Ravishankara and J. F. Stanton,Analysis of the potential atmospheric impact of the reaction of N_2O with OH, *Chem. Phys. Lett.*, 2018, **708**, 100-105.

18. C. A. Cantrell, J. A. Davidson, R. E. Shetter, B. A. Anderson and J. G. Calvert,Reactions of nitrate radical and nitrogen oxide (N_2O_5) with molecular species of possible atmospheric interest, *J. Phys. Chem.*, 1987, **91**, 6017-6021.

19. T. L. Nguyen, M. N. Romanias, A. R. Ravishankara, A. M. Zaras, P. Dagaut and J. F. Stanton,The atmospheric impact of the reaction of N_2O with NO_3: A theoretical study, *Chem. Phys. Lett.*, 2019, **731**, 136605.

20. F. Bernard, G. Eyglunent, V. Daele and A. Mellouki,Kinetics and Products of Gas-Phase Reactions of Ozone with Methyl Methacrylate, Methyl Acrylate, and Ethyl Acrylate, *J. Phys. Chem. A*, 2010, **114**, 8376-8383.

21. H. Chen, Y. Ren, M. Cazaunau, V. Dalele, Y. Hu, J. Chen and A. Mellouki,Rate coefficients for the reaction of ozone with 2-and 3-carene, *Chem. Phys. Lett.*, 2015, **621**, 71-77.

22. G. L. Vaghjiani and A. R. Ravishankara,New measurement of the rate coefficient for the reaction of OH with methane, *Nature*, 1991, **350**, 406-409.

23. A. Mellouki, S. Teton, G. Laverdet, A. Quilgars and G. Le Bras,Kinetic studies of OH reactions with H_2O_2, C_3H_8 and CH_4 using the pulsed laser photolysis - laser induced fluorescence method, *Journal de chimie physique*, 1994, **91**, 473-487.

24. L. Zhou, A. R. Ravishankara, S. S. Brown, M. Idir, K. J. Zarzana, V. Daële and A. Mellouki,Kinetics of the Reactions of NO_3 Radical with Methacrylate Esters, *J. Phys. Chem. A*, 2017, **121**, 4464-4474.

25. L. Zhou, A. R. Ravishankara, S. S. Brown, K. J. Zarzana, M. Idir, V. Daële and A. Mellouki,Kinetics of the reactions of NO_3 radical with alkanes, *Phys. Chem. Chem. Phys.*, 2019, **21**, 4246-4257.

26. H. Fuchs, W. P. Dube, S. J. Cicioira and S. S. Brown,Determination of inlet transmission and conversion efficiencies for in situ measurements of the nocturnal nitrogen oxides, NO_3, N_2O_5 and NO_2, via pulsed cavity ring-down spectroscopy, *Anal. Chem.*, 2008, **80**, 6010-6017.

27. W. P. Dube, S. S. Brown, H. D. Osthoff, M. R. Nunley, S. J. Ciciora, M. W. Paris, R. J. McLaughlin and A. R. Ravishankara,Aircraft instrument for simultaneous, in situ measurement of NO_3 and N_2O_5 via pulsed cavity ring-down spectroscopy, *Rev. Sci. Instrum.*, 2006, **77**.

28. H. Fuchs, W. R. Simpson, R. L. Apodaca, T. Brauers, R. C. Cohen, J. N. Crowley, H. P. Dorn, W. P. Dubé, J. L. Fry, R. Häseler, Y. Kajii, A. Kiendler-Scharr, I. Labazan, J. Matsumoto, T. F. Mentel, Y. Nakashima, F. Rohrer, A. W. Rollins, G. Schuster, R. Tillmann, A. Wahner, P. J. Wooldridge and S. S. Brown,Comparison of N_2O_5 mixing ratios during NO3Comp 2007 in SAPHIR, *Atmos. Meas. Tech.*, 2012, **5**, 2763-2777.

29. J. A. Davidson, A. A. Viggiano, C. J. Howard, I. Dotan, F. C. Fehsenfeld, D. L. Albritton and E. E. Ferguson,Rate constants for reactions of O_2^+, NO_2^+, NO^+, H_3O^+, CO_3^-, NO_2^-, and halide ions with N_2O_5 at 300K, *J. Chem. Phys.*, 1978, **68**, 2085-2087.

30. R. Atkinson, D. L. Baulch, R. A. Cox, J. N. Crowley, R. F. Hampson, R. G. Hynes, M. E. Jenkin, M. J. Rossi, J. Troe and I. Subcommittee,Evaluated kinetic and photochemical data for atmospheric chemistry: Volume II- gas phase reactions of organic species, *Atmos. Chem. Phys.*, 2006, **6**, 3625-4055.

31. G. L. Vaghjiani and A. R. Ravishankara, Photodissociation of H_2O_2 and CH_3OOH at 248 nm and 298 K: Quantum yields for OH, $O(^3P)$ and $H(^2S)$, *J. Chem. Phys.*, 1990, **92**, 996-1003.

Figures:

Figure 1

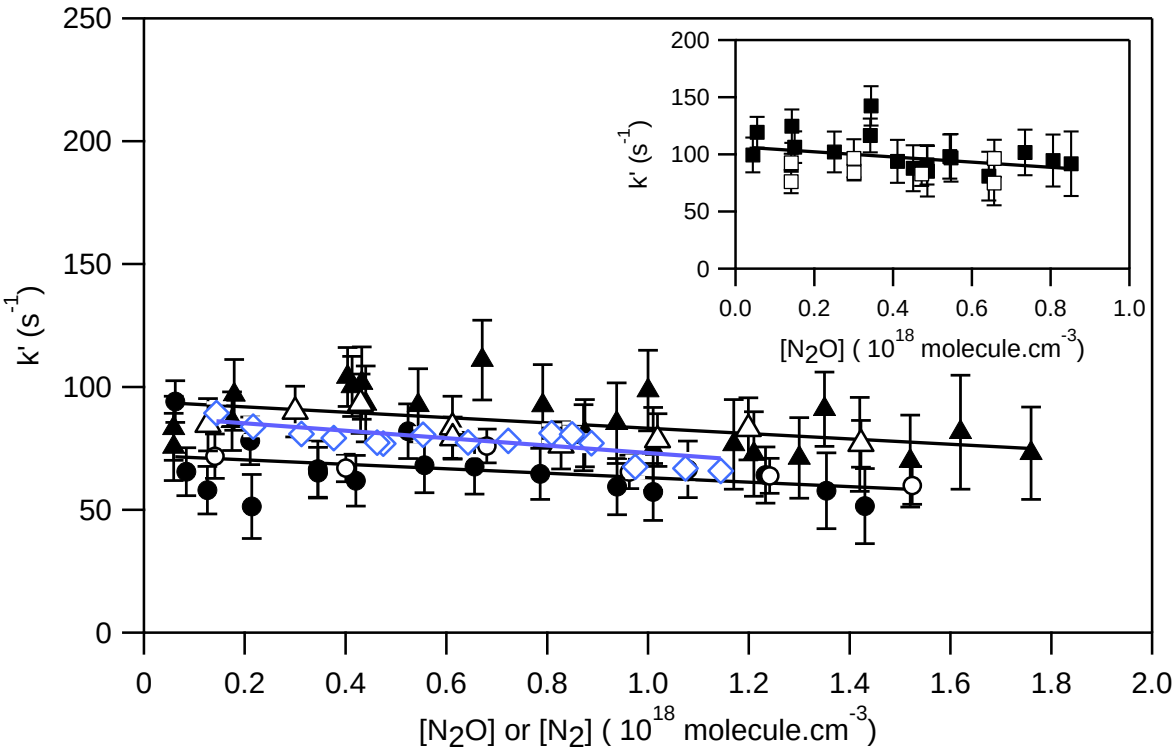

Fig. 1. Pseudo-first order rate coefficients for the loss of OH radicals (k') plotted against the N_2O and N_2 concentrations. The lines represent the linear least-squares fits of data and the slope yields the bimolecular rate coefficient k_1. The filled symbols were obtained in 99% pure N_2O while the open symbols were from 99.998% pure N_2O at 372 K (■ and □), 298 K (▲ and △), and 253 K (● and ○). The obtained values of k_1 at 372, 298, and 253 K are, respectively, $(-2.26 \pm 1.34) \times 10^{-17}$, $(-1.09 \pm 0.34) \times 10^{-17}$ and $(-9.06 \pm 3.91) \times 10^{-18}$ cm^3 $molecule^{-1}$ s^{-1}. The open diamond (◇) represents 298 K data for the addition of N_2, which yields a slope of $(-1.51 \pm 0.38) \times 10^{-17}$ $cm^3.molecule^{-1}.s^{-1}$. The error bars are the 2σ uncertainties from the fits to the individual OH decays plus the estimated systematic error 5% due to uncertainties in measured concentrations of N_2O and N_2.

Figure 2

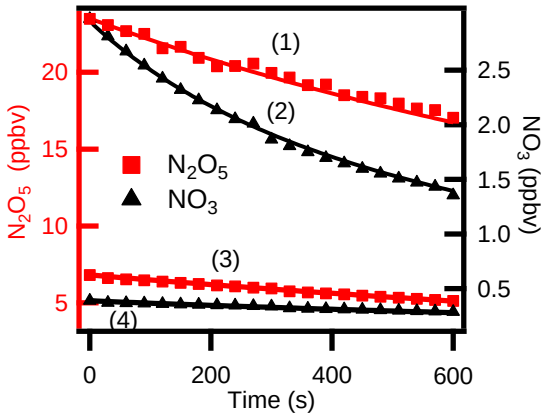

Fig. 2. Observed NO_3 and N_2O_5 mixing ratios (black triangles▲ and red squares ■) and their simulated temporal profiles (lines) before (profiles 1 and 2) and after (profiles 3 and 4) the injection of N_2O into the chamber where NO_3 and N_2O_5 were present at equilibrium. The concentration of N_2O was 5.28×10^{13} molecule cm^{-3}. The fits yield a value of $k_2 = 2.30 \times 10^{-20}$ cm^3 $molecule^{-1}$ s^{-1}. Note that it took a long time (~30 mins) to inject sufficient N_2O into the chamber. During this time NO_3 and N_2O_5 decayed further; however, the signal to noise ratio for the detected species were excellent.